Removal and Binding Energies in Lepton Nucleus Scattering

Arie Bodek, University of Rochester

The 20th International conference on neutrinos from accelerators
NUFAC 2018
WG 2: Thursday Aug 18, 2019

Virginia Tech, Blacksburg, VA
15:30-16:00

https://indico.phys.vt.edu/event/34/sessions/205/#20180816

https://arxiv.org/abs/1801.07975 (to be published in EPJC)

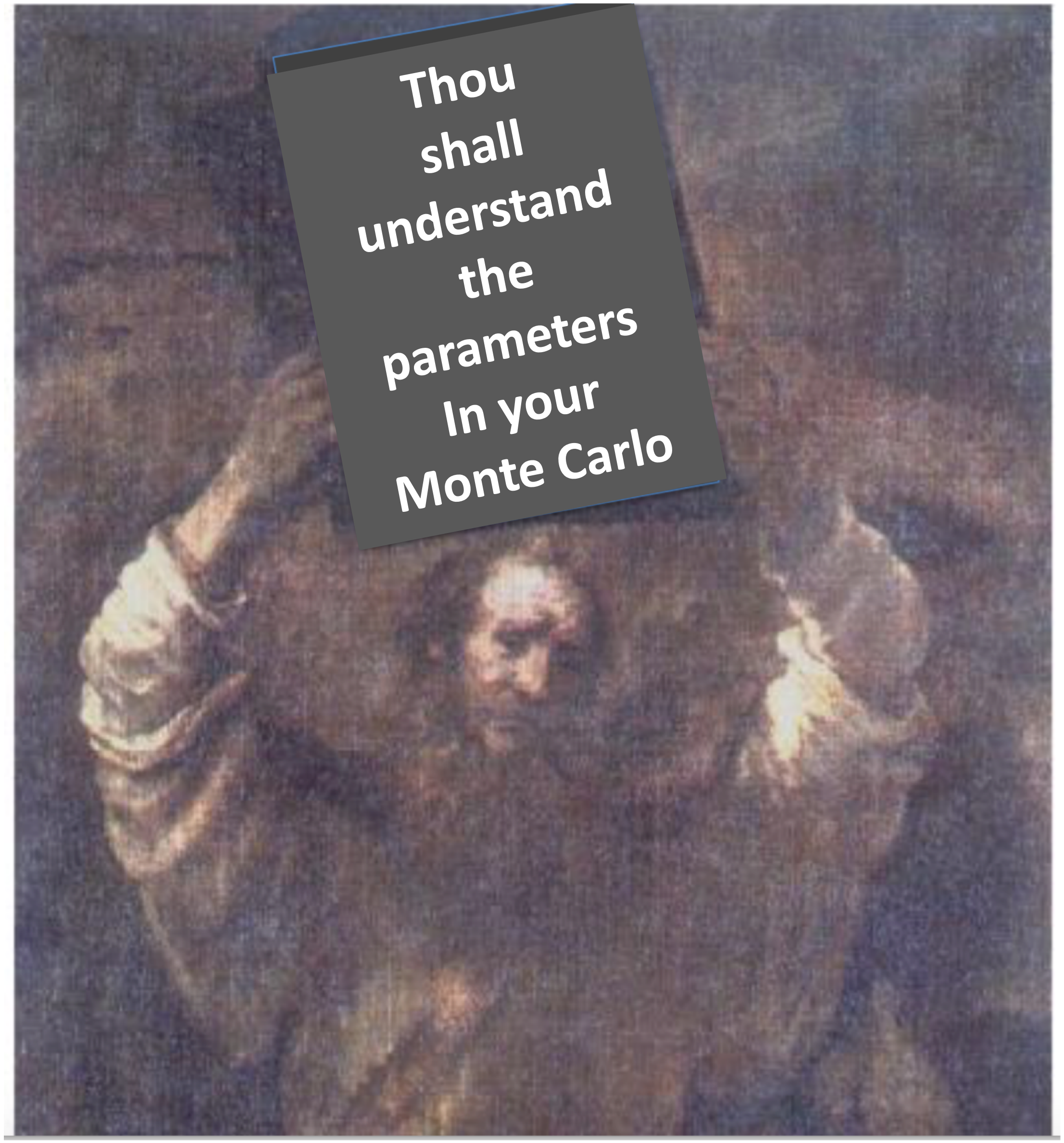
Thou
shall
understand
the
parameters
In your
Monte Carlo

For QE electron scattering the energy momentum δ function and the final state nucleon energy are given by

$$\delta[(E_i + \nu) - E_f]$$
$$E_f = \sqrt{(q+k)^2 + M^2}. \quad (1)$$

$E_i = f(\mathcal{E})$

$\mathcal{E}$ = binding/removal energy parameter

Which is defined differently

in GENIE: Excitation energy $\mathcal{E} = E_x(P,N)$

In NEUT: Smith-Moniz Interaction energy $\mathcal{E} = \epsilon'^{P,N}_{SM}$

other applications: Interaction energy $\mathcal{E} = \epsilon^{P,N}_{R}$

Impulse approx. Spectator A-1 Nucleus

3.1 Excitation energy $[E_x]$ in the Bodek-Ritchie formalism and GENIE

$$E_i^P = M_A - \sqrt{(M_{A-1^*})^2 + k^2}$$

$$M_{A-1^*} = M_{A-1} + E_x^P$$

$$E_i^P = M_A - \sqrt{(M_{A-1} + E_x^P)^2 + k^2}$$

$$E_i^P \approx M_A - \sqrt{(M_{A-1})^2 + k^2} - E_x^P$$

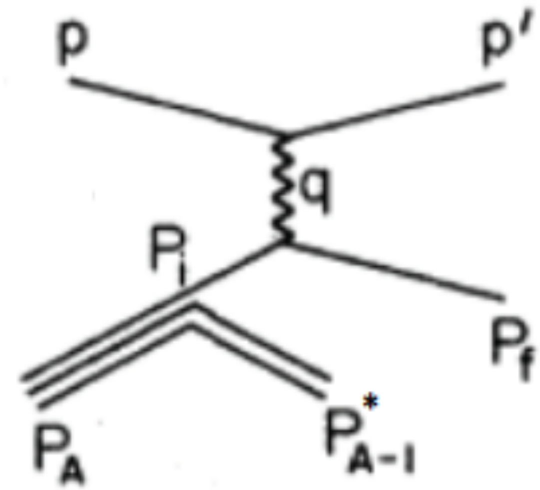

T of A-1*
* = Ex

Recoil A-1* system has kinetic energy T and excitation energy Ex

Ex is the binding energy parameter in the Bodek-Ritchie formalism

Ex is the parameter measured in early ee'P spectral function measurements

GENIE
(Bodek Ritchie 1981)
Used in early spectral function experiments Excitation Energy

$$E_i^P = M_A - \sqrt{(M_{A-1} + E_x^P)^2 + \boldsymbol{k}^2}$$

Modern spectral function experiments ee'P
E_M = Removal or missing energy

$$E_i^P = M_A - \sqrt{(M_A - M + E_m^P)^2 + \boldsymbol{k}^2}.$$

$$M_A = M_{A-1} + M_{p,n} - S^{P,N}$$
$$M_{A-1} = M_A - M_{p,n} + S^{P,N}$$

both Formalisms Conserves momentum & Energy

They are equivalent

$$\langle E_m^P \rangle = S^P + \langle E_x^P \rangle.$$

$S^{P,N}$ =proton (Neutron) separation energy

S (P,N) = Energy it takes to to go from **grounds state** of atomic mass A to ***ground state*** of A-1 nucleus.
Sp is tabulated in nuclear mass tables.

$^{A}_{Z}Nucl$	remove proton	S^P	remove neutron	S^N
	Spectator		Spectator	
$^{2}_{1}$H	N	2.2	P	2.2
$^{6}_{3}$Li 1+	$^{5}_{2}$He $\frac{3}{2}$-	4.4	$^{5}_{3}$Li $\frac{3}{2}$-	5.7
$^{12}_{6}$C 0+	$^{11}_{5}$B $\frac{3}{2}$-	16.0	$^{11}_{6}$C $\frac{3}{2}$-	18.7
$^{16}_{8}$O 0+	$^{15}_{7}$N $\frac{1}{2}$-	12.1	$^{15}_{8}$O $\frac{1}{2}$-	15.7
$^{24}_{12}$Mg 0+	$^{23}_{11}Na$ $\frac{3}{2}$+	11.7	$^{23}_{12}$ Mg $\frac{3}{2}$+	16.5
$^{27}_{13}$Al$\frac{5}{2}$+	$^{26}_{12}Mg$ 0+	8.3	$^{23}_{12}$ Al 5+	13.1
$^{28}_{14}$Si 0+	$^{27}_{13}$Al$\frac{5}{2}$+	11.6	$^{27}_{14}$Si $\frac{5}{2}$+	17.2
$^{40}_{18}$Ar$\frac{3}{2}$+	$^{39}_{17}$CL $\frac{3}{2}$+	12.5	$^{39}_{18}$Ar $\frac{7}{2}$-	9.9
$^{40}_{20}$Ca 0+	$^{39}_{19}$K $\frac{3}{2}$ +	8.3	$^{39}_{20}$Ca $\frac{3}{2}$+	15.6
$^{51}_{23}$V $\frac{7}{2}$-	$^{50}_{22}$Ti 0+	8.1	$^{50}_{23}$V 6+	11.1
$^{56}_{26}$Fe 0+	$^{55}_{25}$Mn $\frac{5}{2}$ -	10.2	$^{55}_{26}$Fe $\frac{3}{2}$-	11.2
$^{58}_{28}$Ni $\frac{3}{2}$ -	$^{58}_{27}$Co 2+	8.2	$^{58}_{87}$Ni 0+	12.2
$^{89}_{39}$Y $\frac{1}{2}$ -	$^{88}_{38}$Sr $\frac{1}{2}$-	7.1	$^{88}_{39}$Y 4-	11.5
$^{90}_{40}$Zr 0+	$^{89}_{39}$Y $\frac{1}{2}$ -	8.4	$^{88}_{40}$Zr$\frac{9}{2}$+	12.0
$^{120}_{50}$Sn 0+	$^{119}_{49}$In $\frac{9}{2}$ +	10.1	$^{119}_{50}$Sn $\frac{1}{2}$+	8.5
$^{181}_{73}$Ta$\frac{7}{2}$ -	$^{180}_{72}$Hf 0+	5.9	$^{180}_{73}$Ta 1+	7.6
$^{197}_{79}$Au$\frac{3}{2}$+	$^{196}_{78}$Pt 0+	5.8	$^{196}_{79}$Au 2-	8.1
$^{208}_{82}$Pb 0+	$^{207}_{81}$TI $\frac{1}{2}$+	8.0	$^{207}_{82}$Pb $\frac{1}{2}$-	7.4

Table 1. The spin parity transitions and separation energies S^P, S^N and S^{N+P} when a proton or a neutron or both are removed from various nuclei. All energies are in MeV.

S (P,N) is tabulated in nuclear mass tables

Carbon

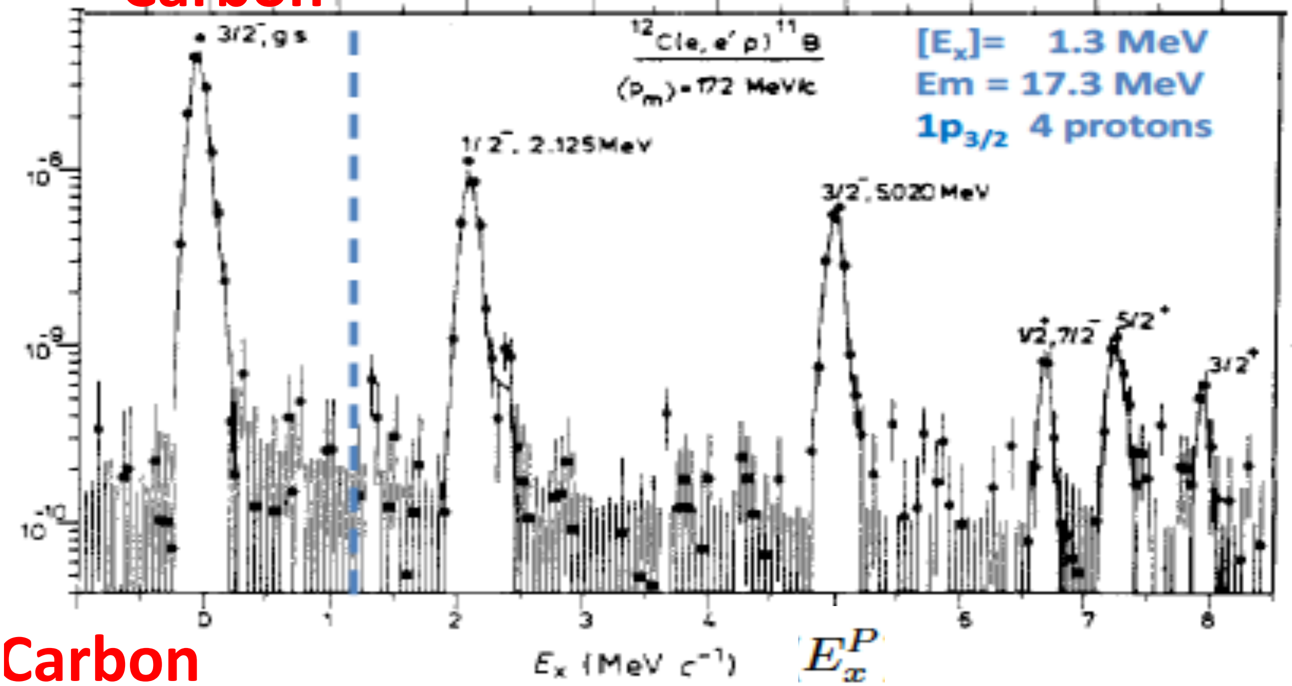

E_x^P

1P (1/2)

ee'P high resolution 1p1h
Here Ex is measured

$$\langle E_m^P \rangle = S^P + \langle E_x^P \rangle .$$

Carbon

Sp=16 MeV

ee'P high resolution 1p1h
here Em is measured

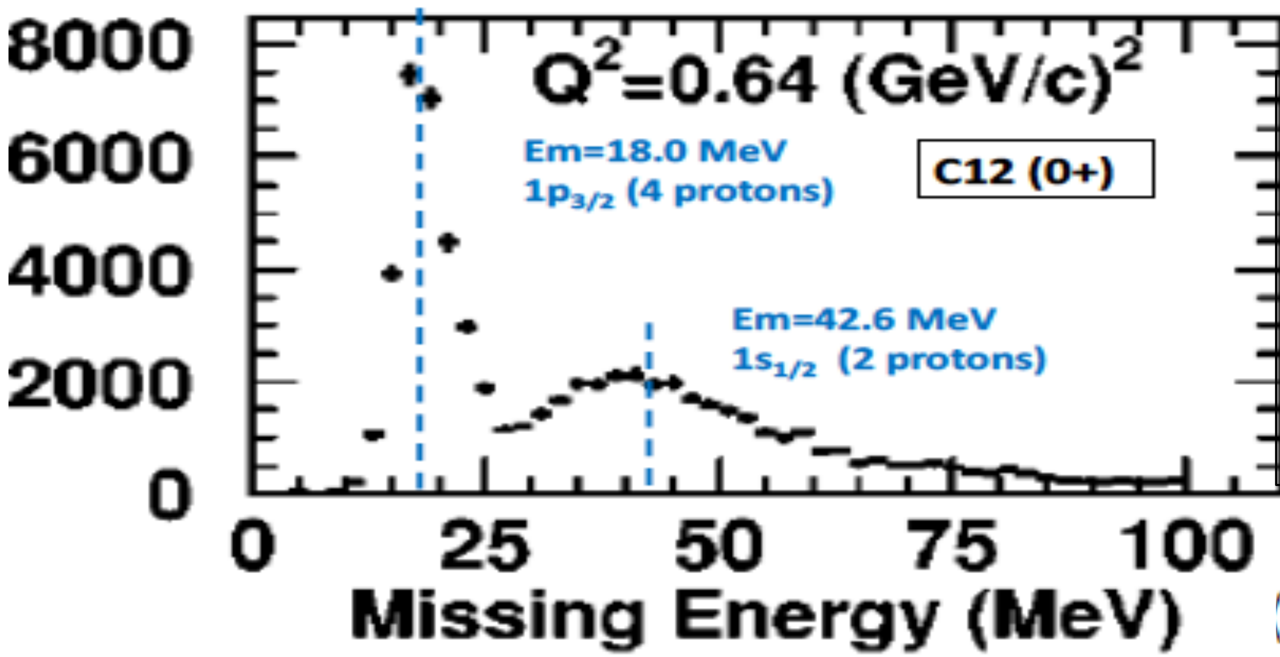

E_m^P

Define peak or most probable value as [Em]

Define average as <Em>
For neutrino experiments

2p2h Em>80 GeV)

Bodek-Ritchie
GENIE
2p2h process
High momentum short
range correlations

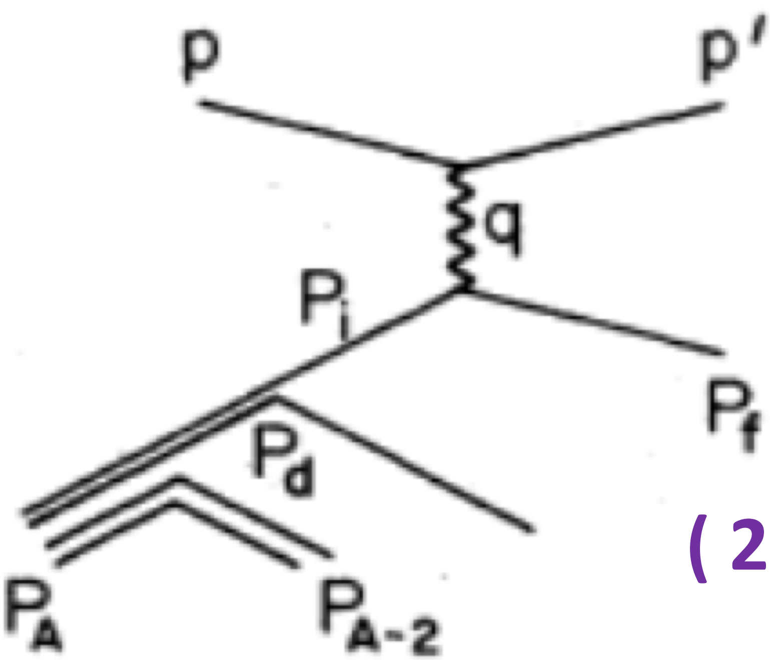

(2p2h Em>80 GeV)

Fig. 4. 2p2h process: Scattering from an off-shell bound proton of momentum p_i=k from two nucleon short range correlations (quasi-deuteron). There is an on-shell spectator (A-2) * nucleus and an on-shell spectator recoil neutron with momentum $-k$. The off-shell energy of the interacting bound proton is $E_i^P(SRC) = M_D - \sqrt{M_n + k^2} - \Delta_{SRC}^{N+P}$.

The 2p2hg process typically has missing energy more than 80 MeV.

Should be calculated separately from 1p1h (high momentum tail from short range correlations)

Em e e'P measurements of level removal energy

Nucleus S^P		$^{12}_{6}C$ 16.0	Carbon		
ee′p $\epsilon_R^P = E_m + T_{A-1}$		shell removal energy E_m^P Saclay	shell removal energy E_m^P NIKHEF	shell removal energy E_m^P Tokyo	width FWHM Tokyo
$1s_{1/2}$	2	38.1±1.0	42.6±5	36.9±0.3	19.8±0.5
$1p_{3/2,1/2}$	4	17.5±0.4	17.3±0.4	15.5±0.1	6.9±0.1
$1d_{5/2,3/2}$ $2s_{1/2}$ $1f_{7/2}$					
T_{A-1}		1.4	1.4	1.4	
Mean $\langle E_m^P \rangle^{levels}$	6	**$\langle 24.4 \pm 2 \rangle$**	**$\langle 25.7 \pm 2 \rangle$**	**$\langle 22.6 \pm 3 \rangle$**	
levels removed		1s	1s	1s	
$[E_m^P]^{levels}_{1s}$	4	[17.5±1]	[17.3±0.4]	[15.5±1]	
Peak $[E_m^P]^{levels}_{1s1p}$					
$[E_m^P]^{levels}_{est}$	4	[17.5±1]	[17.3±0.4]	[15.5±1]	
difference $\langle E_m \rangle^{levels} - [E_m]^{levels}_{est}$		**6.9±3**	**8.4±3**	**7.1±3**	(ave) **(7.3)**

Table 5. Results of a DPWA analysis of the "level removal energies" for different shell-model levels done by the Saclay[26] and Tokyo[27–29] $ee'p$ experiments on $^{12}_{6}C$, $^{28}_{14}Si$ and $^{58}_{28}Ni$. Also shown are results of our re-analysis of the Moniz[10] data. Values of the [*peak*] are shown in square brackets and values for the ⟨*mean*⟩ are shown in angular brackets.

Calculating average removal energy from level removal energy measured in ee'P

Em e e'P measurements of level removal energy

Carbon

Nucleus S^P	$^{12}_{6}C$ 16.0					$^{28}_{14}Si$ 11.6		$^{58}_{28}Ni$ 8.2	
ee′p $\epsilon_R^P = E_m + T_{A-1}$		shell removal energy E_m^P Saclay	shell removal energy E_m^P NIKHEF	shell removal energy E_m^P Tokyo	width FWHM Tokyo		shell removal energy E_m^P Saclay		shell removal energy E_m^P Saclay
$1s_{1/2}$	2	38.1±1.0	42.6±5	36.9±0.3	19.8±0.5	2	51.0	2	62.0
$1p_{3/2,1/2}$	4	17.5±0.4	17.3±0.4	15.5±0.1	6.9±0.1	6	32.0	6	45.0
$1d_{5/2,3/2}$						4	16.1±0.8	10	21.0
$2s_{1/2}$						2	13.8±0.5	2	14.7±0.2
$1f_{7/2}$								8	9.3±0.3
T_{A-1}		1.4	1.4	1.4			0.7		0.4
$\langle E_m^P\rangle^{levels}$	6	**⟨24.4 ± 2⟩**	**⟨25.7 ± 2⟩**	**⟨22.6 ± 3⟩**		14	**⟨27.6 ± 2⟩**	28	**⟨25.3 ± 2⟩**
levels removed		1s	1s	1s			1s or 1s1p		1s or 1s1p
$[E_m^P]^{levels}_{1s}$	4	[17.5±1]	[17.3±0.4]	[15.5±1]		12	[23.7±1]	26	[22.5±1]
$[E_m^P]^{levels}_{1s1p}$						6	[15.3±1]	20	[15.7±1]
$[E_m^P]^{levels}_{est}$	4	[17.5±1]	[17.3±0.4]	[15.5±1]		9	[19.5±4.2]	23	[19.1±3.4]
difference $\langle E_m\rangle^{levels} - [E_m]^{levels}_{est}$		**6.9±3**	**8.4±3**	**7.1±3**	(ave) (7.3)		**8.1±4.2**		**6.2±3.4**

Mean

Peak

Table 5. Results of a DPWA analysis of the "level removal energies" for different shell-model levels done by the Saclay[26] and Tokyo[27–29] $ee'p$ experiments on $^{12}_{6}C$, $^{28}_{14}Si$ and $^{58}_{28}Ni$. Also shown are results of our re-analysis of the Moniz[10] data. Values of the [*peak*] are shown in square brackets and values for the ⟨*mean*⟩ are shown in angular brackets.

Calculating average removal energy from level removal energy measured in ee'P

3.4 Interaction energy $\epsilon_R^{P,N}$

= Em plus kinetic energy of recoil A-1* system

The fully relativistic expression for the interaction energy ϵ_R^P of a proton is defined as:

Used for: $Q^2_{QE\text{-}\mu}$ $E_\nu^{QE\text{-}\mu}$:

$$E_i^P = M - \epsilon_R^P. \tag{8}$$

For

$$E_i^P = M_A - \sqrt{(M_A - M + E_m^P)^2 + k^2}, \tag{9}$$

we obtain

$$\begin{aligned} \epsilon_R^P &= {E_m}^P + T_{A-1} \\ &= S^P + E_x + T_{A-1}. \end{aligned} \tag{10}$$

Here, $T_{A-1} = \sqrt{k^2 + M_{A-1}^2} - M_{A-1}$ is the kinetic energy of the recoiling (A-1) spectator nucleus.

$$\delta[(E_i + \nu) - E_f]$$

$$E_f = \sqrt{(q+k)^2 + M^2}.$$

3.6 The Smith-Moniz formalism

Different definition of E_i

Smith and Moniz [5] use on-shell relativistic kinematics as follows,

include kinetic on shell

compensate with larger binding

$$E_i = (k^2 + M_{p,n}^2)^{1/2} - \epsilon_{SM}^{\prime P,N}.$$

Compare to $$E_i^P = M - \epsilon_R^P.$$ (interaction energy)

$$\epsilon_{SM}^{\prime P,N} = \epsilon_R^{P,N} + T_{av}$$

Smith-Moniz Interaction energy

$$T_{av}^P = \langle (k^2 + M_p^2)^{1/2} - M_p \rangle$$

$$\approx \frac{\langle k^2 \rangle}{2M_p}.$$

non-relativistic approximation
(only correct on average)

Symbol	
$E_x^{P,N}$	Spectator Nucleus Excitation Used in spectral functions implemented in GENIE[1]
$S^{P,N}$ $= M_{A-1} + M_{p,n} - M_A$	Separation Energy Nuclear Data Tables (measured) [19, 20]
$E_m^{P,N} = S^{P,N} + E_x^{P,N}$	removal (or missing) energy used in spectral functions
$\epsilon_R^{P,N} = E_m^{P,N} + T_{A-1}$ $T_{A-1} =$ $= \sqrt{k^2 + M_{A-1}^2} - M_{A-1}$ $\approx \frac{k^2}{2M_{A-1}}$	interaction energy is $\epsilon_R^{P,N}$ $E_i = M - \epsilon_R^{P,N}$ used in $E_\nu^{QE-\mu}$, $Q^2_{QE-\mu}$, and Q^2_{QE-P}, also used in effective spectral functions[8]
$\epsilon_{SM}^{\prime(P,N)} = \epsilon_R^{P,N} + T_{av}^{P,N}$ $T = \sqrt{k^2 + M^2} - M$ $\langle k^2 \rangle = 0.6 K_F^2$	$\epsilon_{SM}^{\prime(P,N)}$ is Smith Moniz[11] Interaction energy $E_i = M + T - \epsilon_{SM}^{\prime(P,N)}$ used in NEUT-NUANCE[3, 4]

<Peak] vs <Mean>

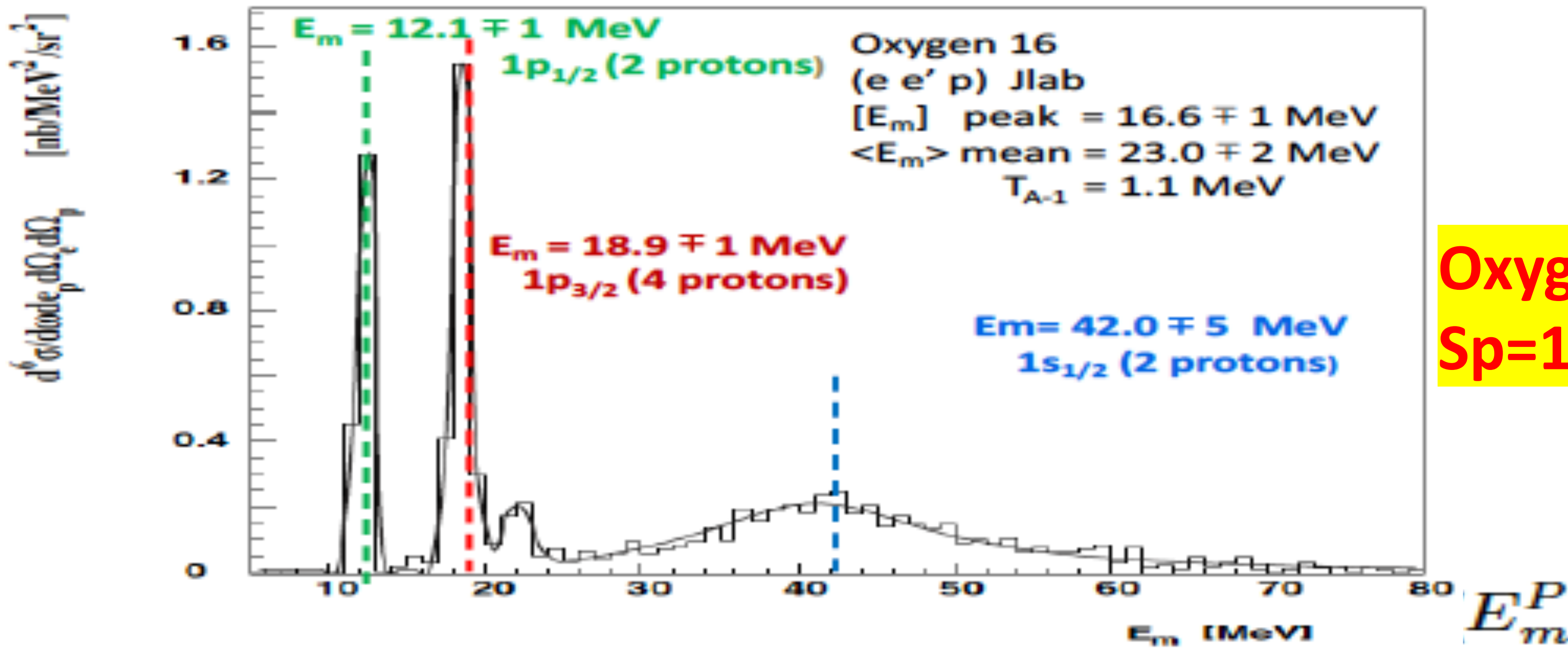

Oxygen
Sp=12.1 MeV

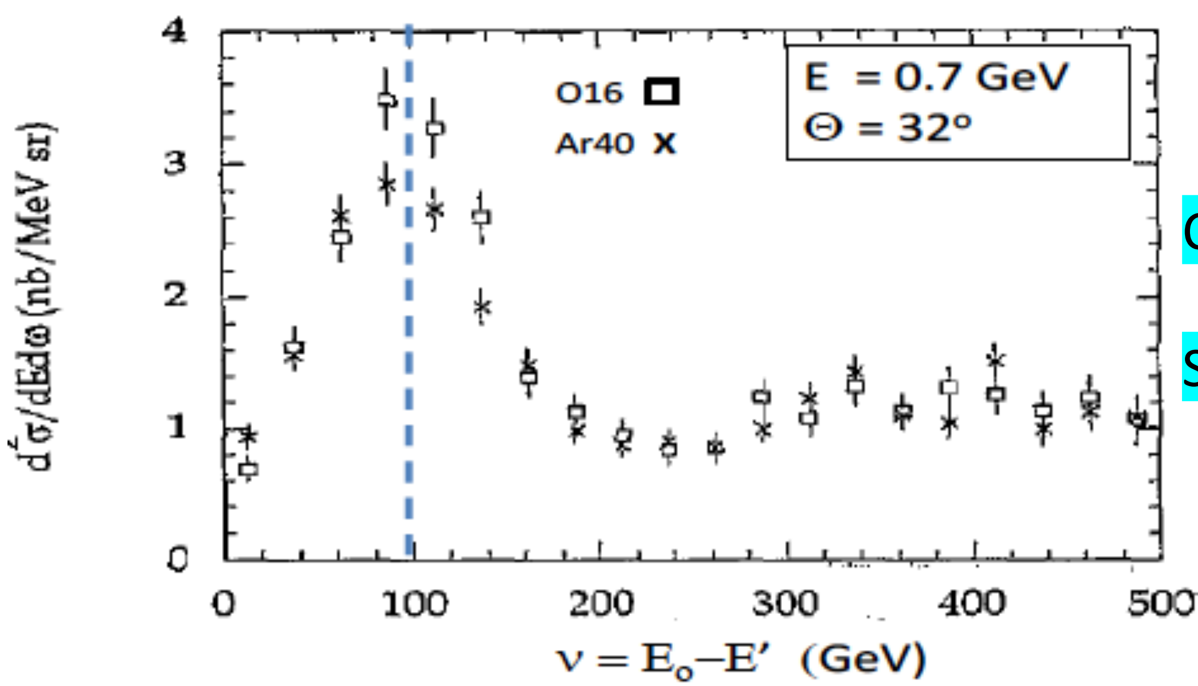

Compare oxygen and argon

Single arm ep>e'X

We can extract interaction and removal energy parameters from electron scattering data from a variety of modern experiments in three different ways.

Best $\overline{\langle E_m^P \rangle}^{SF}$

1. The *mean* removal energy extracted for tests of the Kotlun[15] sum rule from $ee'p$ spectral functions.

2nd Best $\langle E_m^P \rangle^{levels}$

2. The *mean* removal energy extracted from the weighted average of the removal energies of shell-model energy levels as measured in $ee'p$ experiments. **EM levels**

Not as good

3. The location of the QE *peak* in inclusive e-A scattering (e.g. Moniz et. al.) with additional corrections described below.

All should agree if done correctly

5.1 Direct measurements of $\langle E_m^P \rangle^{SF}$ and $\langle T \rangle^{SF}$

Koltun Sum rule

These two quantities are directly extracted from spectral function measurements in analyses that test the Koltun sum rule [12]. The Koltun's sum rule states that

$$\frac{E_0}{A} = \frac{1}{2}\left[\langle T \rangle^{SF} \frac{A-2}{A-1} - \langle E_m^P \rangle^{SF}\right], \quad (34)$$

where E_0/A is the nuclear binding energy per particle obtained from nuclear masses and includes a (small) correction for the Coulomb energy,

$$\langle T \rangle^{SF} = \int d^3k \; dE_m \; \frac{k^2}{2M} P_{SF}(k, E_m) \; , \quad (35)$$

Ave. < KE>

and

$$\langle E_m \rangle^{SF} = \int d^3k \; dE_m \; E_m \; P_{SF}(k, E_m) \; . \quad (36)$$

Ave. $<E_m>$

Exactly what we need For momentum distribution And binding

For precise tests of the Koltun sum rule a small contribution from three-nucleon processes should taken into account.

Koltun Sum rule measurements

Target	Q2	$\langle T \rangle$ $E_m^P < 80$	$\langle E_m \rangle$ $E_m^P < 80$
$^{12}_{6}$**C** Jlab Hall C [22]	0.6	15.9	26.0
	1.2	16.3	25.8
	1.8	16.0	26.6
	3.2	17.3	26.2
Jlab $\langle T \rangle^{SF}$, $\langle E_m^P \rangle^{SF}$	Ave.	16.4±0.6	**26.1±0.4**
Saclay $\langle T \rangle^{SF}$,$\langle E_m^P \rangle^{SF}$		16.9±0.5	23.4±0.5
Saclay $\langle E_m^P \rangle^{levels}$			24.4±2
K_F=221±5		15.5 ±1.2	

Compare to Fermi gas

Target	Q2	$\langle T \rangle$	$\langle E_m \rangle$
$^{28}_{14}$**Si**			
Saclay $\langle T \rangle^{SF}$, $\langle E_m^P \rangle^{SF}$		17.0±0.6	**24.0±0.6**
Saclay $\langle E_m^P \rangle^{levels}$			27.6±2
K_F=239±5		18.1±1.3	

Compare to Fermi gas

Target	Q2	$\langle T \rangle$	$\langle E_m \rangle$
$^{40}_{20}$**Ca**			
Saclay $\langle T \rangle^{SF}$, $\langle E_m^P \rangle^{SF}$		16.6±0.5	**27.8±0.5**
Saclay$\langle E_m^P \rangle^{levels}$			26.5±2
K_F=239±5		18.1±1.3	

Target	Q2	$\langle T \rangle$	$\langle E_m \rangle$
$^{56}_{26}$**Fe**	0.6	20.4	30.7
Jlab Hall C [22]	1.2	18.1	29.4
	1.8	17.8	27.8
	3.2	19.1	28.8
Jlab $\langle T \rangle^{SF}$, $\langle E_m^P \rangle^{SF}$	Ave.	18.8±1.0	**29.2±1.1**
K_F=254±5		20.4±1.4	

Target	Q2	$\langle T \rangle$	$\langle E_m \rangle$
$^{58}_{28}$**Ni**			
Saclay $\langle T \rangle^{SF}$,$\langle E_m^P \rangle^{SF}$		18.8±0.7	**25.0±0.7**
Saclay$\langle E_m^P \rangle^{levels}$			25.3±2
K_F=257±5		20.9±1.4	

Target	Q2	$\langle T \rangle$	$\langle E_m \rangle$
$^{197}_{79}$**Au**	0.6	20.2	25.5
Jlab Hall C [22]	1.2	18.4	25.7
	1.8	18.3	24.1
	3.2	19.4	26.1
Jlab $\langle T \rangle^{SF}$, $\langle E_m^P \rangle^{SF}$	Ave.	19.1±0.8	**25.3±0.8**
K_F=245±5		19.0±1.3	

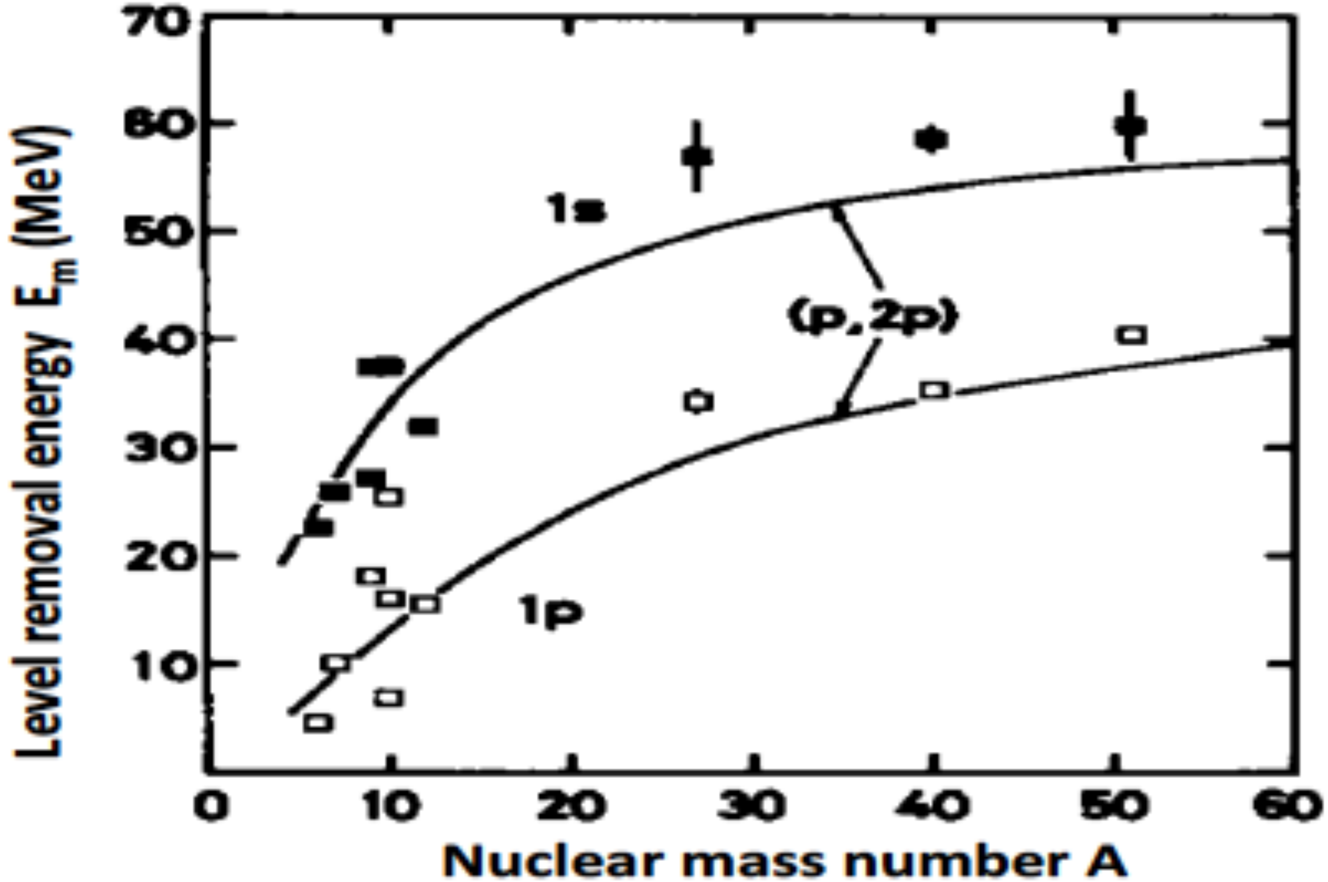

Fig. 4. Single "level removal energies" $\langle E_m^P \rangle^{1s}$ and $\langle E_m^P \rangle^{1p}$ for the 1s and 1p states, respectively. The data points are measurements done in $ee'p$ experiments [26]. The solid curves represent interpolations of the "level removal energies" observed in (p, 2p) experiments [27]. The "level removal energies" for the 1s and 1p states measured in $ee'p$ experiments are systematically higher than those observed in (p, 2p) experiments.

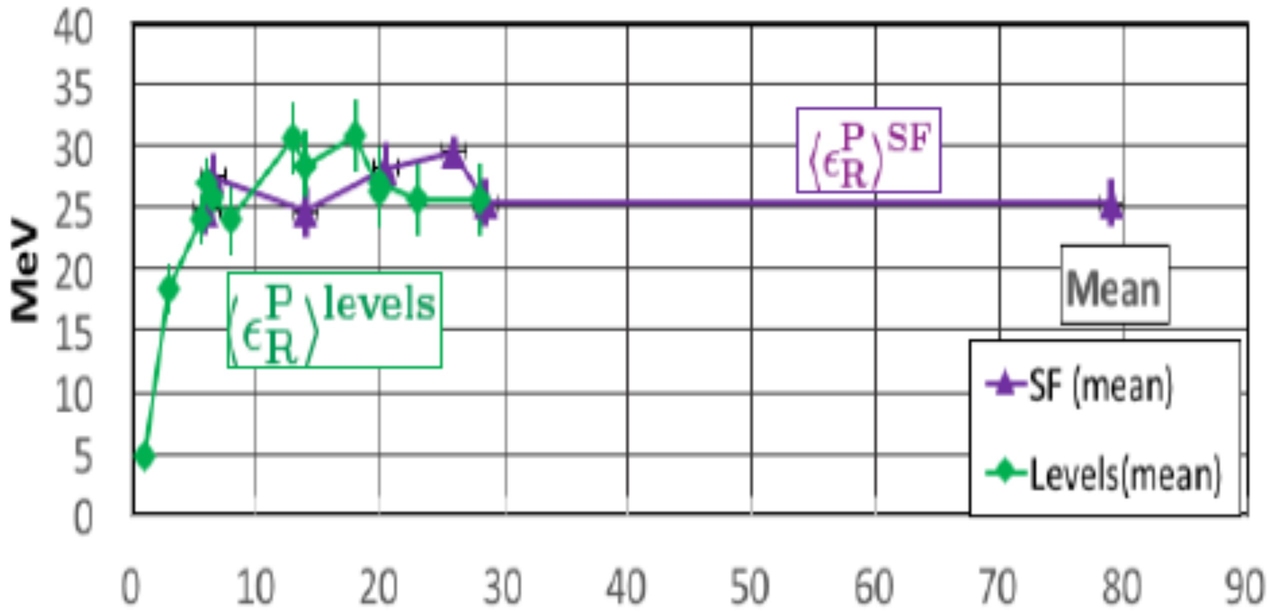

SF = Koltun sum rule from Spectral Function

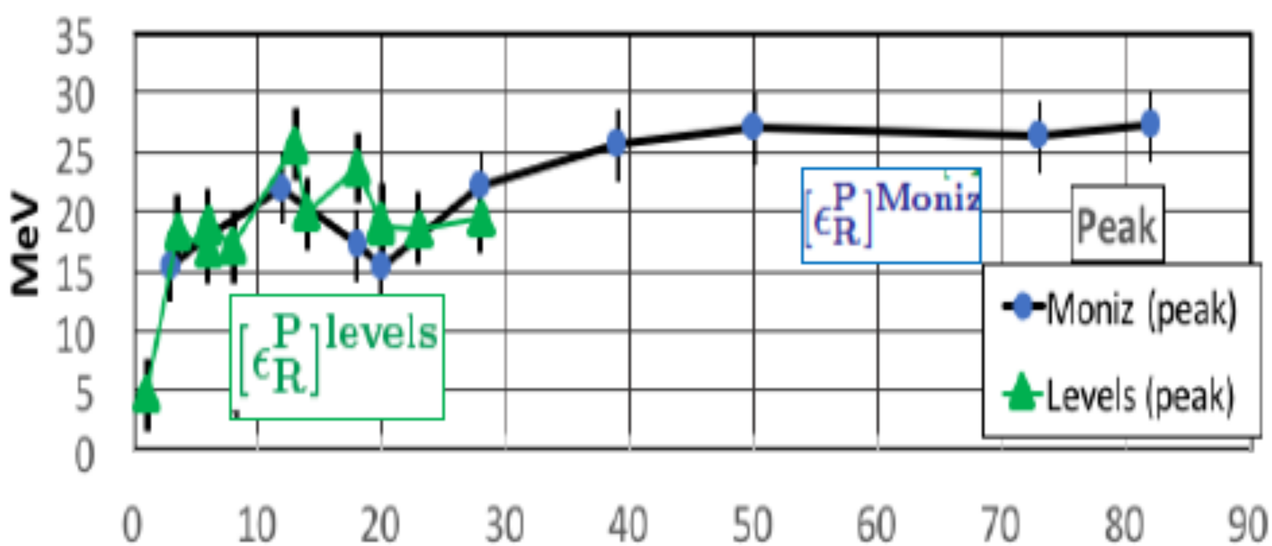

Here, we corrected Moniz for Coulomb and Relativistic kinematics

Values of the [*peak*] are shown in square brackets a

values for the ⟨*mean*⟩ are shown in angular brackets.

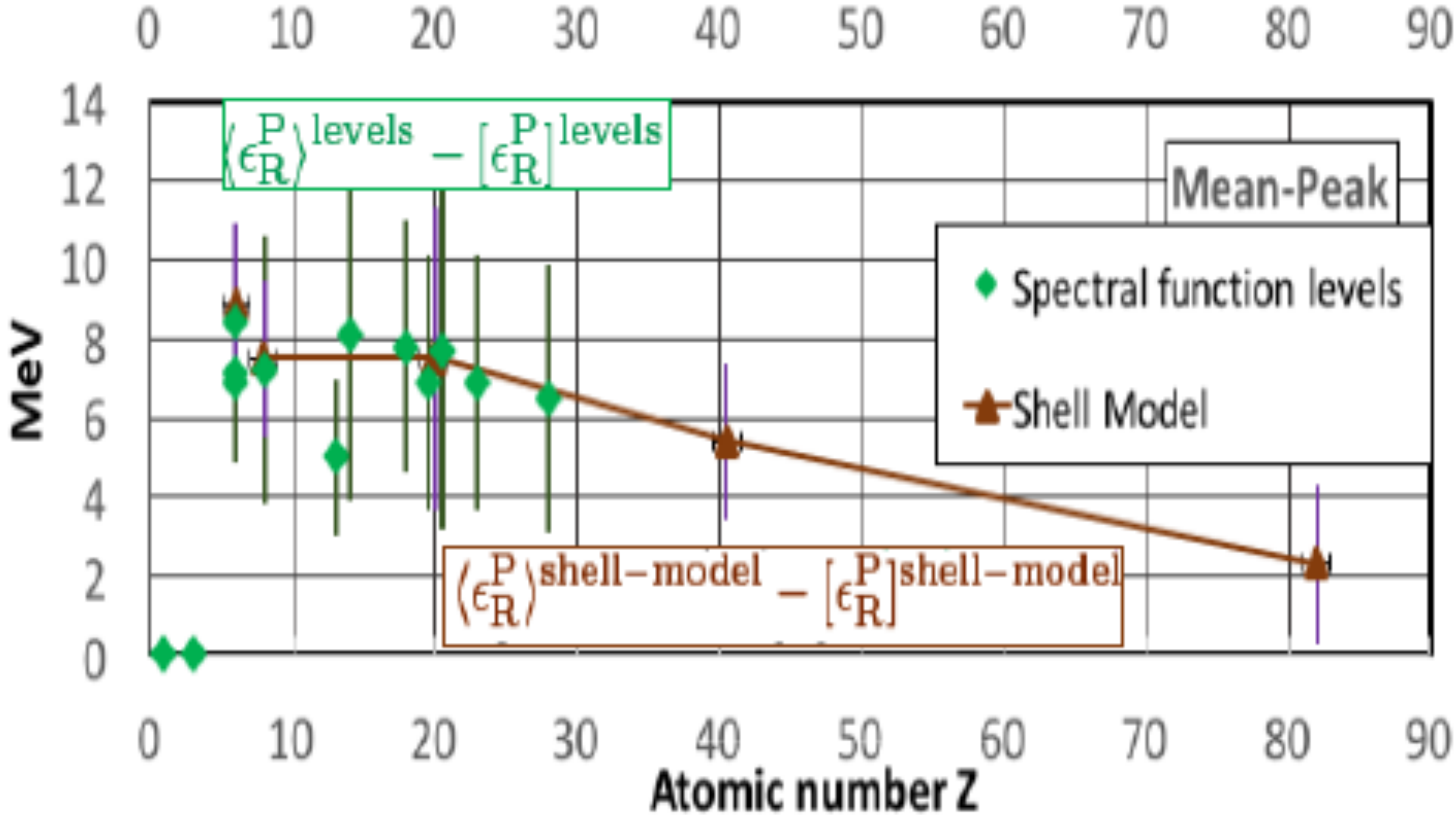

$\langle\epsilon_R^P\rangle^{levels} - [\epsilon_R^P]^{levels}$
Mean-Peak
Spectral function levels
Shell Model
$\langle\epsilon_R^P\rangle^{shell-model} - [\epsilon_R^P]^{shell-model}$
MeV
Atomic number Z

$Q^2_{QE\text{-}\mu}$ $E_\nu^{QE\text{-}\mu}$

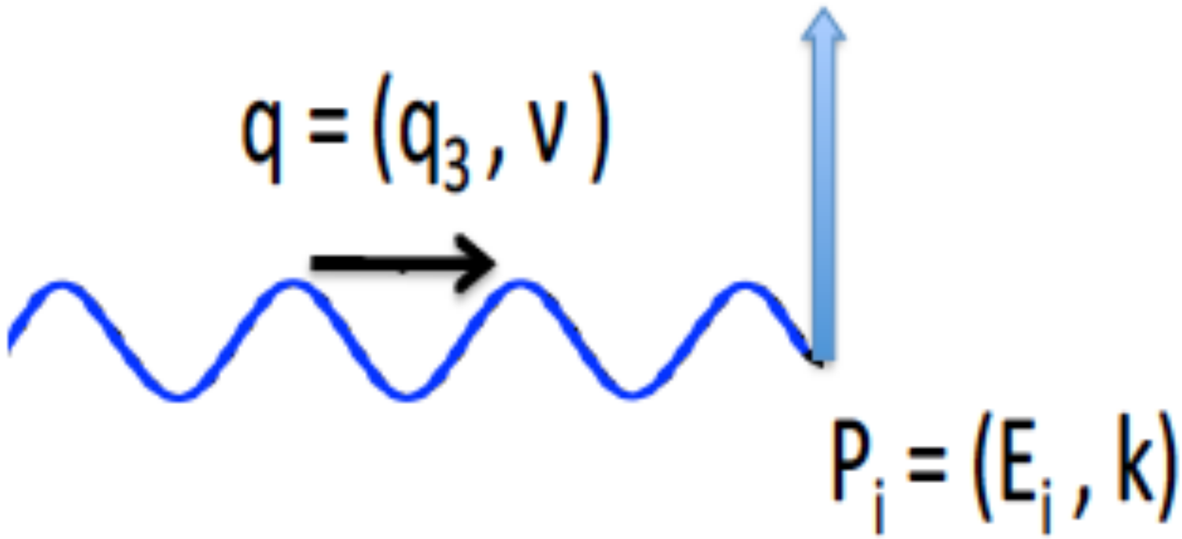

Fig. 3. Scattering from an off-shell bound nucleon of momentum k which is perpendicular to the direction of the virtual photon. This is the configuration at the *peak* of the Fermi motion smearing. At the *peak* of the distribution the z component of the nucleon momentum (k_z) is zero.

For neutrino QE scattering we define $E'_{\mu\text{-}} = T_{\mu\text{-}} + m_\mu + |V_{eff}|$ as the total Coulomb corrected muon energy. The adjusted bound neutron energy in the laboratory system is $M'_n = M_n - \langle \epsilon_R^N \rangle$. We define $(M'_p)^2 = M_p^2 + \langle k^2_{T\text{-}N} \rangle$ to account for the fact that the final state proton has the same average transverse momentum as that of the initial state neutron $\langle k^2_{T\text{-}N} \rangle$ with respect to the neutrino-muon scattering plane. From energy-momentum conservation we get:

$$E_\nu^{QE\text{-}\mu} = \frac{2(M'_n)E'_{\mu\text{-}} - ((M'_n)^2 + m_\mu^2 - (M'_p)^2)}{2 \cdot [(M'_n) - E'_{\mu\text{-}} + (\sqrt{(E'_{\mu\text{-}})^2 - m_\mu^2}) \cos\theta_{\mu\text{-}}]} \quad (39)$$

$$Q^2_{QE\text{-}\mu} = -m_\mu^2 + 2E_\nu^{QE}(E'_{\mu\text{-}} - \sqrt{(E'_{\mu\text{-}})^2 - m_\mu^2} \cos\theta_{\mu\text{-}}).$$

$$Q^2_{QE\text{-}P} = (M'_n)^2 - (M'_p)^2 + 2M'_n[M_p + T_p - M'_n].$$

Should use these updated equations with the correct interaction energy.y
If we set Veff=0, K_T=0, and use wrong interaction energy, then we get what is currently being used.

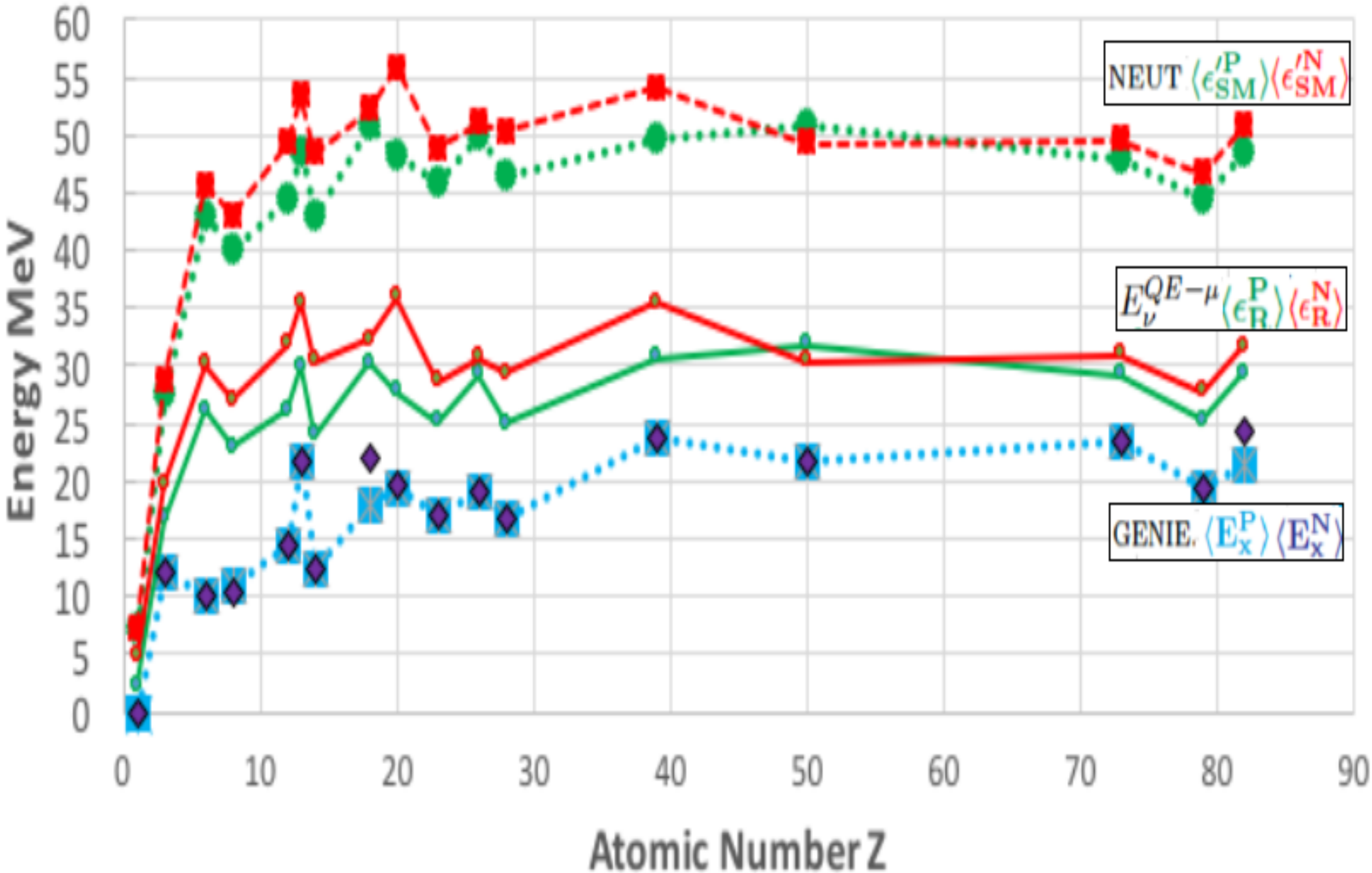

People have been using 27 MeV for Carbon. Genie users should use 10 MeV, Neut users should use 46 MeV

People have been using 27 MeV for Carbon.

Genie users should use 10 MeV, Neut users should use 46 MeV

Binding energy is the largest systematic error in Δm^2_{32}

The two-neutrino transition probability can be written as

$$P_{\nu_\alpha \to \nu_\beta}(L) = \sin^2 2\vartheta \, \sin^2 \left(1.27 \, \frac{(\Delta m^2/\mathrm{eV}^2)\,(L/\mathrm{km})}{(E_\nu/\mathrm{GeV})} \right).$$

The location of the first oscillation maximum in neutrino energy ($E_\nu^{1st-min}$) is when the term in brackets is equal to $\pi/2$. An estimate of the extracted value of Δm^2 is given by:

$$\Delta m^2 = \frac{2E_\nu^{1st-min}}{1.27\pi L}. \qquad (2)$$

For example, for the T2K experiment[12] $L = 295\ Km$, and E_ν is peaked around 0.6 GeV. The T2K experiment[12] reports a value of

$$\Delta m^2_{32} = (2.434 \pm 0.064) \times 10^{-3}\ \mathrm{eV}^2.$$

S. Dennis, talk at Nufact 2018, Virginia Tech, Blacksburg,

A 15 MeV change in binding energy yields a change in the extracted value of Δm^2_{32} of

$0.031 \times 10^{-3}\ \mathrm{eV}^2$

With our analysis the binding energy uncertainty is 3 MeV so this error is reduced by a factor of 5

Combined analysis:
Christoph Andreas Ternes
Nufact 2018

Δm^2_{32} **=(2.50 +- 0.03)**$\times 10^{-3}\ \mathrm{eV}^2$

Need to make sure that binding Energy is treated consistently Between experiments.

Red is of interest to neutrino experiments: carbon, oxygen, argon, calcium, iron, lead

$^A_Z Nucl$	$\langle \epsilon_R^{P,N} \rangle$ relativ. corected		$\langle \epsilon_{SM}^{\prime P,N} \rangle$ SMITH-MONIZ	$\langle E_x^{P,N} \rangle$ BODEK-RITCHIE	
	$E_m + T_{A-1}^{P,N}$		$\epsilon_R^{P,N} + T$	$E_m^{P,N}$-$S^{P,N}$	
	use for $E_\nu^{QE-\mu}$ $Q^2_{QE-\mu}$ Q^2_{QE-P} $\langle \epsilon_R^P \rangle$	$\langle \epsilon_R^N \rangle$	used in **NEUT** interaction energy $\langle \epsilon_{SM}^{\prime P} \rangle$,$\langle \epsilon_{SM}^{\prime N} \rangle$	used in **GENIE** excitation energy $\langle E_x^P \rangle$,$\langle E_x^N \rangle$	Measurment method used
(^2_1H)	4.7	4.7	7.2, 7.2	0.0, 0.0	Binding energy
^6_3Li	18.4±3	19.7 ±3	27.5, 28.8	12.2, 12.2	$\langle \epsilon_R \rangle^{levels}$ Tokyo [24, 25, 26]
$^{12}_6C$	27.5±3	30.1±3	43.0, 45.6	10.1, 10.0	Koltun SR $\langle \epsilon_R \rangle^{SF}$ Jlab Hall C [22]
$^{16}_8O$	24.1±3	27.0±3	40.1, 43.0	10.9, 10.2	$\langle \epsilon_R \rangle^{levels}$ Jlab Hall A [28]
$^{24}_{12}Mg$	27.0±3	31.8±3	44.5, 49.3	14.5, 14.5	updated $\langle \epsilon_R^P \rangle^{Moniz}$ [4]
$^{27}_{13}Al$	30.6±3	35.4±4	48.5, 53.3	21.6, 21.6	$\langle \epsilon_R \rangle^{levels}$ Tokyo [24, 25, 26]
$^{28}_{14}Si$	24.7±3	30.3±3	42.8, 48.4	12.4, 12.4	Koltun SR $\langle \epsilon_R \rangle^{SF}$ Saclay [23]
$^{40}_{18}Ar$	30.9±4	32.3±4	50.8, 52.2	17.8, 21.8	$\langle \epsilon_R \rangle^{levels}$ Tokyo [24, 25, 26] +Shell model
$^{40}_{20}Ca$	28.2±3	35.9±4	48.1, 55.8	19.4, 19.8	Koltun SR $\langle \epsilon_R \rangle^{SF}$ Saclay [23]
$^{50}_{23}V$	25.6±3.	28.6±4	45.8, 48.8	17.0, 17.0	$\langle \epsilon_R \rangle^{levels}$ Tokyo [24, 25, 26]
$^{56}_{26}Fe$	29.6±3	30.6±3	50.0, 51.0	19.0, 19.0	Koltun SR $\langle \epsilon_R \rangle^{SF}$ Jlab Hall C [22]
$^{58.7}_{28}Ni$	25.4±3	29.4±3	46.3, 50.3	16.8, 16.8	Koltun SR $\langle \epsilon_R \rangle^{SF}$ Saclay [23]
$^{89}_{39}Y$	31.0±3	35.4±3	49.7, 54.1	23.6, 23.6	updated $\langle \epsilon_R^P \rangle^{Moniz}$ [4]
$^{118.7}_{50}Sn$	32.0±3	30.4±3	50.9, 49.3	21.7, 21.7	updated $\langle \epsilon_R^P \rangle^{Moniz}$ [4]
$^{181}_{73}Ta$	29.3±3	31.0±3	47.8, 49.5	23.3, 23.3	updated $\langle \epsilon_R^P \rangle^{Moniz}$ [4]
$^{197}_{79}Au$	25.4±3	27.7±3	44.4, 46.7	19.5, 19.5	Koltun SR $\langle \epsilon_R \rangle^{SF}$ Jlab Hall C [22]
$^{208}_{82}Pb$	29.5±3	31.7±3	48.5, 50.7	21.4, 24.2	updated $\langle \epsilon_R^P \rangle^{Moniz}$ [4]

Corrections to Moniz Measurements

Appendix

e-A expt.	$^{A}_{Z}$ Nucl.	K_F^P,K_F^N Moniz ±5 MeV/c	K_F^P ψ'[13] fit	$E_{\rm shift}$ ψ'[13] fit MeV	$[\epsilon_M^P]$ pub. Moniz MeV	$\lvert V_{eff}\rvert$ Gueye ref.[14] MeV	$[\epsilon_{cc}^P]$ Coul. corrctd MeV	$[\epsilon_R{}^P]$ relativ. corrctd [*peak*]	⟨*mean*⟩ minus [*peak*] est.	$\langle\epsilon_R{}^P\rangle$ relativ. corrctd ⟨*mean*⟩
Moniz[10]	$^{6}_{3}Li$	169,169	165	15.1	17±3	1.4	16.3	15.4±3	0.0	15.4±3
Moniz	$^{12}_{6}C$	221,221	228	20.0	25±3	3.1±0.25	23.6	18.0±3	7.3±2	25.3±4
Moniz	$^{24}_{12}Mg$	235,235	230	25.0	32±3	4.8	29.4	22.0±3	(5.0 ±3)	27.0±4
Frascati[22]	$^{40}_{18}Ar$	251,263		-	-	6.6	-	17.2±5	7.8±3.4	25.0±5
Moniz	$^{40}_{20}Ca$	251,251	241	28.0	28±3	7.4±0.6	24.6	15.4±3	7.3±3.2	22.7±5
Moniz	$^{58.7}_{28}Ni$	257,269	245	30.0	36±3	9.8	31.9	22.1±3	6.5±3.4	28.6±5
Moniz	$^{89}_{39}Y$	243,263	245		39±3	11.6	33.6	25.6±3	(5.4±3)	31.0±4
Shell-model	$^{90}_{40}Zr$	243,263	-		-		-	-	5.4±3	-
Moniz	$^{118.7}_{50}Sn$	245,270	245	28.0	42±3	13.6	35.0	27.0±3	(5.0±3)	32.0±4
jlab[14]	$^{154}_{64}Gd$	245,272	-		-	15.9±1.2	-	-	-	-
Moniz	$^{181}_{73}Ta$	242,271	245		42±3	17.3	33.9	26.3±3	(3.0±3)	29.3±4
Moniz	$^{208}_{82}Pb$	245,277	248	31.0	44±3	18.9±1.5	35.2	27.2±3	2.3±3	29.5±4

Table 3. A summary of our re-extractions of the interaction energy parameters from the Moniz[10] analysis. Also shown are results for $^{40}_{18}Ar$ from the Frascati[22] e-A inclusive experiment. All energies are in MeV. For details see section 4.13.